Nanoscale Advances

ROYAL SOCIETY OF CHEMISTRY

PAPER

View Article Online
View Journal | View Issue

Cite this: *Nanoscale Adv.*, 2023, **5**, 1386

A facile cost-effective electrolyte-assisted approach and comparative study towards the Greener synthesis of silica nanoparticles†

Arighna Saha,[ac] Kritika Narula,[b] Prashant Mishra,[b] Goutam Biswas *[a] and Snehasis Bhakta *[c]

Nowadays, silica nanoparticles are gaining tremendous importance because of their wide applications across different domains such as drug delivery, chromatography, biosensors, and chemosensors. The synthesis of silica nanoparticles generally requires a high percentage composition of organic solvent in an alkali medium. The eco-friendly synthesis of silica nanoparticles in bulk amounts can help save the environment and is cost-effective. Herein, efforts have been made to minimize the concentration of organic solvents used during synthesis *via* the addition of a low concentration of electrolytes, *e.g.*, NaCl. The effects of electrolytes and solvent concentrations on nucleation kinetics, particle growth, and particle size were investigated. Ethanol was used as a solvent in various concentrations, ranging from 60% to 30%, and to optimize and validate the reaction conditions, isopropanol and methanol were also utilized as solvents. The concentration of aqua-soluble silica was determined using the molybdate assay to establish reaction kinetics, and this approach was also utilized to quantify the relative concentration changes in particles throughout the synthesis. The prime feature of the synthesis is the reduction in organic solvent usage by up to 50% using 68 mM NaCl. The surface zeta potential was reduced after the addition of an electrolyte, which made the condensation process faster and helped reaching the critical aggregation concentration in a shorter time. The effect of temperature was also monitored, and we obtained homogeneous and uniform nanoparticles by increasing the temperature. We found that it is possible to tune the size of the nanoparticles by changing the concentration of electrolytes and the temperature of the reaction using an eco-friendly approach. The overall cost of the synthesis can also be reduced by ~35% by adding electrolytes.

Received 30th November 2022
Accepted 25th January 2023

DOI: 10.1039/d2na00872f

rsc.li/nanoscale-advances

1. Introduction

The widespread application of silica nanoparticles in the domains of drug delivery, chromatography, biosensors and chemosensors[1–4] demands a robust, efficient method for the synthesis of highly monodisperse, spherical, colloidal silica nanoparticles. The synthesis of silica nanoparticles extensively depends upon the hydrolysis of silicon alkoxide/TEOS by ammonia catalysis and subsequent condensation of the silanol monomer. These two processes are collectively known as Stöber's method of silica nanoparticle synthesis.[5] The growth of nanoparticles is generally described by two models: first one is the monomer addition where primary seed formation by TEOS hydrolysis is the initial stage, followed by the growth of the seed by the deposition of hydrolyzed silanol monomer over it.[6,7] Another method is the aggregation-only model, where simply aggregating the primary seed followed by surface attachment of silanol monomer leads to the particle growth.[8,9] The monomer addition model explains the monodispersed particle synthesis at high ammonia concentrations and the aggregation-only model describes the polydisperse particle synthesis at lower concentrations of ammonia.[10,11] Han *et al.*[12] supported the growth mechanism by proposing two pathways. Pathway I is the incubation stage where the nucleation/growth of the silica particle is determined by TEOS hydrolysis and pathway II is the size enlargement of the silica particle *via* condensation, simply by adding the newly formed silica monomer. Ammonia-catalyzed particle synthesis is time-consuming and most of the synthesis requires 7–24 h.[13–15] Bhakta *et al.*[16] employed a NaOH-catalyzed method and observed a quick polymerization and growth process that eliminated the particle seeding behavior.

[a]*Department of Chemistry, Cooch Behar Panchanan Barma University, Cooch Behar, West Bengal, India 736101. E-mail: goutam@cbpbu.ac.in*

[b]*Department of Biochemical Engineering and Biotechnology, Indian Institute of Technology Delhi, New Delhi, India 110016*

[c]*Department of Chemistry, Cooch Behar College, Cooch Behar, West Bengal, India 736101. E-mail: snehasisbhakta@coochbeharcollege.org.in*

† Electronic supplementary information (ESI) available. See DOI: https://doi.org/10.1039/d2na00872f

Various solvents and solvent mixtures were utilized in the cited literature to investigate the influence of polarity on the kinetics of hydrolysis and condensation. As the polarity of the protic solvent increases, the strength of H-bonding with the hydroxyl group increases, slowing the hydrolysis of TEOS. Thus, methanol as a solvent should be responsible for the slowest rate and going towards the higher branched alcohols should make it faster. Another factor is the steric effect, which completely opposes the previous statement meaning that methanol having the smallest alkyl group contributes least to the steric hindrance and makes the hydrolysis process faster; these two theories are contradictory.[17,18] Atul *et al.*[19] worked with different organic solvents starting from short-chain to long-chain carbon to understand the role of solvents in kinetics in a wide range and reported that the rates of hydrolysis and condensation are fastest in a ~1 : 1 mixture of ethanol : decanol and are slowest in pure ethanol. This indicates that on lowering the polarity of the solvent medium, the rates of hydrolysis and condensation increase. The size of the nanoparticle also depends on the solvent polarity; a less polar solvent, *i.e.*, ethanol and decanol in a 1 : 1 mixture gives a larger particle of around 2 μm and only ethanol gives particles of less than 500 nm.[19] Delyan *et al.*[20] reported that solvent polarity plays a crucial role in the nucleation and growth of nanoparticles. Diluting TEOS with the co-solvent (ethanol, butanol, isopropanol, and cyclohexane) affects the monomer transfer rate at the organic/aqueous interface. Solvents with low polarity where the phase separation is higher due to poor solvation of TEOS, lower the transfer rate and finally lower the supersaturation concentration, which is responsible for the larger particle size and refers to the secondary nucleation theory.[20]

The added electrolyte in the reaction mixture creates a crucial effect on particle size. The increased ionic strength of the solution promotes particle coagulation.[21] The adsorption of cationic species on silica nanoparticles reduces the surface potential and thus promotes the aggregation of the silanol monomer at the initial reaction stage. Highly monodispersed micrometer-sized particles were synthesized by using LiCl, NaCl, and KCl and the order of sizes of silica particles in presence of electrolyte was LiCl < NaCl < KCl.[21] Thus, adding electrolytes to the solvent mixture can increase the rate of formation of silica nanoparticles. In terms of the industrial production of silica nanoparticles, a green, sustainable[22] and low-cost[23] synthesis would be highly accomplished. Therefore, we tried to decrease the concentration of organic solvent during the synthesis, which would be environmentally friendly as well as cost-effective.

Despite the abundance of literature on silica nanoparticle synthesis and detailed analysis in different solvent systems, to our best knowledge, there have been no reports on the effect of depleted organic solvent in the synthesis. The most common method and widely used industrial synthesis for silica nanoparticles is the Stöber method. The main drawback of this method is that it requires a high amount of ammonium hydroxide as the base and a higher reaction time. There are lots of green methods[22,24,25] in which extracted natural resources are used to synthesize the silica nanoparticle and other metal and non-metal-based nanoparticles are employed but herein, we have developed a chemical method involving NaOH-catalyzed silica nanoparticle synthesis in the presence of electrolytes to minimize the use of organic solvents in the reaction medium to make it eco-friendly as well as industry-friendly. To understand the particle growth phenomenon, we varied the solvent composition, starting from a higher solvent concentration to a lower one, and compared the particle growth rate and size distribution of electrolytic as well as non-electrolytic processes. The correlation between the final particle size distribution and solvent properties was depicted, and we established a trend in order of size, stability, and polydispersity by changing the solvent and solvent compositions. Different organic solvents, *e.g.*, ethanol, methanol, and propanol, were employed and with the addition of a very low concentration of NaCl, we were able to reduce the organic solvent content significantly to obtain

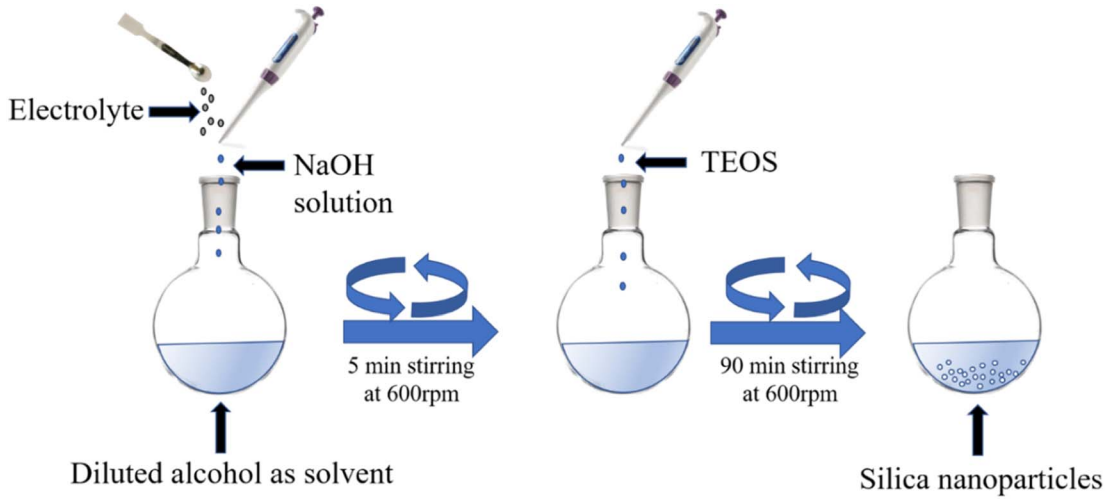

Scheme 1 Schematic representation of silica nanoparticle synthesis using an electrolyte.

monodisperse silica nanoparticles. The particles were thoroughly characterized and the kinetics of the growth was also established to understand the mechanism using the molybdate assay by measuring the soluble silica concentration. Using different electrolytes like LiCl, NaCl, KCl, and CsCl, we compared the sizes of the particles and tried to understand the roles of different electrolytes during particle growth. The sizes of SiNP are tunable with varying electrolyte concentrations (Scheme 1).

2. Experimental

2.1 Materials

Tetraethyl orthosilicate (TEOS 98%, Sigma Aldrich), sodium hydroxide (NaOH, Loba Chemie), sodium chloride (NaCl, Merck), ethanol (99%), methanol (99%, Rankem), isopropanol (SRL Chemicals), Milli-Q water and all other reagents were used without further purification.

2.2. Synthesis

The synthesis of silica nanoparticles was carried out in different alcoholic (ethanol, methanol, and propanol) medium with concentrations ranging from 60% to 30%, using NaOH as the base catalyst. The NaOH-assisted reaction mainly proceeds *via* the initial rapid nucleation of silicic acids followed by a condensation pathway to produce white nanoparticles. Different amounts of electrolytes were mixed and the optimized amount of the electrolytes was used to synthesize particles, especially at the lower concentration of the alcoholic solution. To obtain the 16 mM concentration of NaOH, 200 μL of 2 N NaOH was mixed with 20 mL of alcoholic solution in a 100 mL round-bottom flask. The mixture was then agitated at 600 rpm for 5 min, and finally 400 μL TEOS was added to the mixture to obtain the 90 mM TEOS concentration. The reaction was performed for 90 min. at a stirring speed of 600 rpm. Then, NaCl, as an electrolyte, was added in catalytic amounts to the solvent composition of 40% and 30% ethanol and the optimized concentrations of the electrolyte were 0.034 M and 0.068 M as given in Table S1, ESI.†

2.3. Analysis of silicic acid/soluble silica concentration change by molybdate assay

The silica precursors, *i.e.*, monomers, dimers, and trimers of ethoxy silane and unreacted TEOS, are collectively known as soluble silica. During the synthesis of silica nanoparticles, this soluble silica concentration was measured at a specific time interval.[22] A 500 μL sample was taken from the reaction mixture and centrifuged for 2–3 min at 3500 rpm to settle the silica nanoparticles. The supernatant containing the soluble silica was then treated with 250 μL of 0.265 M ammonium molybdate, 250 μL (1 N) HCl, 250 μL (0.27 M) Na_2EDTA to get a straw-yellow color of silicomolybdic acid. After 10 min, this silicomolybdic acid was treated with 250 μL of 0.67 M tartaric acid and finally, it was reduced to a blue colored compound by adding a 500 μL of 1.35 M sodium sulfite (Fig. S1†). The absorbance of the blue-colored solution was measured using a UV-Vis spectrophotometer (Thermo Fisher Evolution 201) at a maximum wavelength of 690–700 nm.[26]

2.4. Particle size analysis

The white SiNP was collected by centrifugation at 3500 rpm for 5–6 min, washed three times with deionized water, and finally with ethanol. The particles were dried for 5 h at 60–70 °C in a vacuum oven. The colloidal form of nanoparticles was used for the particle size distribution (PSD) study by dynamic light scattering (Anton Parr Litesizer 500), and size by transmission electron microscopy (TEM, JEOL JEM-1400). The dried particles were used for characterization by Fourier transform infrared spectroscopy (FTIR) in ATR mode (Nicolet iS50, Thermo Fisher).

3. Results and discussion

3.1. Characterization

TEM images (Fig. 1a) of SiNPs synthesized using 50% ethanol showed that the particles were highly monodisperse and their sizes were in between 700–800 nm. The FT-IR spectra (Fig. 1b) were obtained for the SiNP synthesized using 50% ethanol in the absence of electrolyte and 40%, 30% ethanol with electrolyte. All the spectral patterns had similar absorption peaks, and strong bands were observed at 1100 cm^{-1} for asymmetric stretching and at 800 cm^{-1} for the symmetric stretching of Si–O–Si.[27] The crystalline phase of the sample was determined by XRD measurements (Rigaku Ultima-IV). Radial scans of intensity *versus* scattering angle (2θ) were recorded from 5° to 80°. The X-ray diffraction of silica showed a peak at 22.5° in both the nanoparticles (Fig. 1c), which is typical for amorphous silica.[28,29]

3.2. Growth and PSD analysis

In order to minimize the concentration of alcohol as well as the amount of base used for the SiNP synthesis, we envisioned that the synthetic route designed for the SiNP favors condensation over hydrolysis under mild basic conditions where NaOH as a catalyst helps in the nucleation process and the solvent assists the burst nucleation by achieving the critical aggregation concentration (CAC) of silicic acid. As discussed previously, alcohol concentration plays a vital role in TEOS solvolysis. TEOS is soluble in concentrated alcoholic solvents, while on diluting the solvent, it phases out and affects the monomer or silicic acid generation. According to Bhakta *et al.*, in 1 : 1 aqueous ethanolic solvent in the presence of NaOH, hydrolysis becomes faster. In the first 20 min, the concentration of hydroxyl ion decreases rapidly, which suggests that NaOH acts as a catalyst and helps in nucleation followed by the condensation process.[16] Nucleation and growth of the particle are two integral parts of this condensation process. Our experiments suggest that in a diluted alcoholic solvent like 40%, 30%, and so on, the silicic acid changes its concentration slowly (Fig. 2a), and fails to achieve the quick CAC/supersaturation point where no such siloxane network/cluster leads to the formation of primary seed and ultimately ends up with 'no particle' generation. This

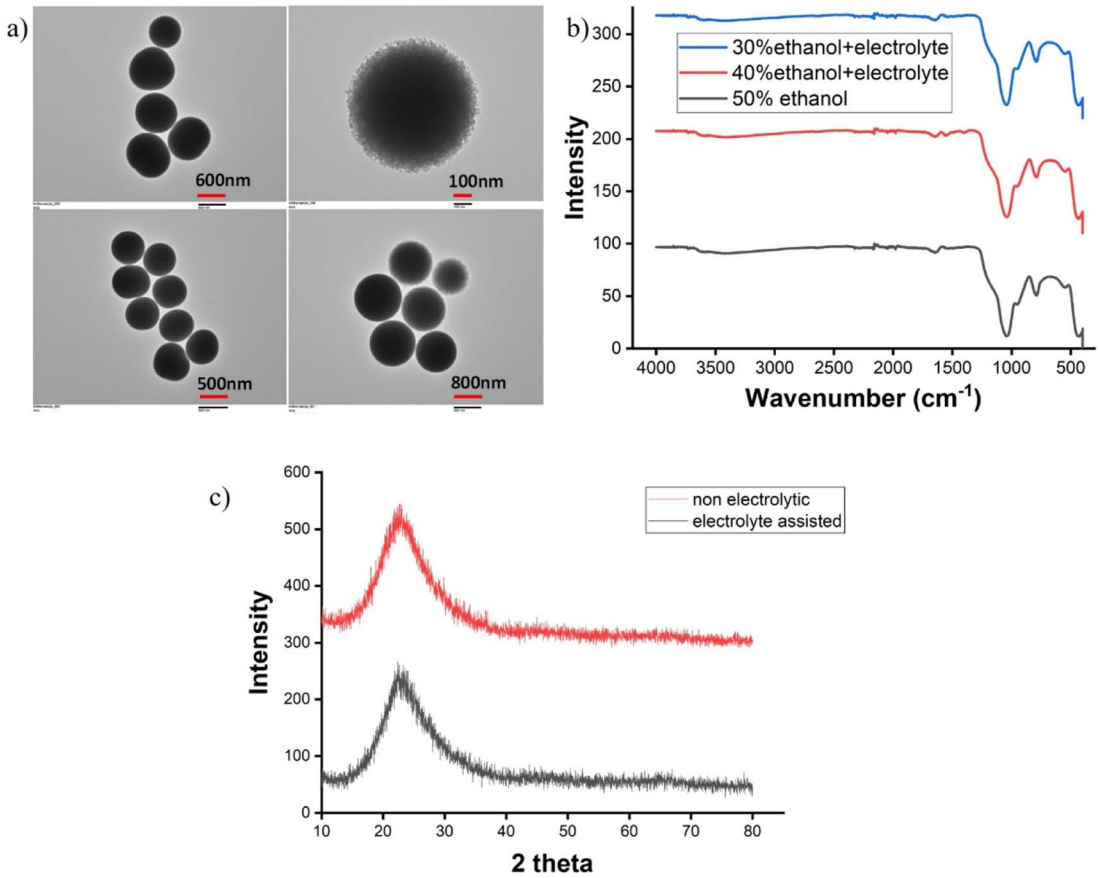

Fig. 1 Characterization of silica nanoparticles (a) TEM analysis of SiNPs synthesized using optimized electrolytic concentrations. (b) FTIR spectra of SiNPs synthesized using electrolytic and non-electrolytic pathways in different compositions of ethanol. (c) XRD patterns of SiNPs synthesized using electrolyte and non-electrolyte-assisted pathways.

problem regarding primary nucleation, especially in the case of 30% and 40% alcoholic solvent, has been solved by using an electrolyte. The nanoparticle formation study by molybdate assay (Fig. S1†) gives higher C_{NP}/C_{SA} values as compared to the non-electrolytic process (Fig. 2b). This refers to high nucleation rate with particle formation.

C_{NP} = (conc. of initial silicic acid − conc. of silicic acid in specific time) = concentration of nanoparticles. C_{SA} = concentration of initial silicic acid.

The homogeneity in particle size distribution is maximum in the case of 60% ethanolic solvent, and going towards the diluted environments like 50%, 40%, and 30%, the

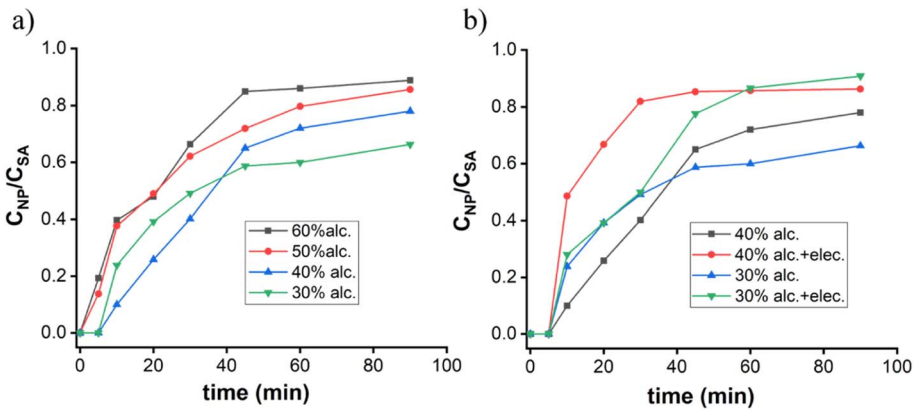

Fig. 2 (a) Changes in the relative concentration of silica nanoparticles with time. Varying the ethanol concentration from 60% to 30%. (b) Comparing the electrolytic and non-electrolytic processes in 30% and 40% ethanol.

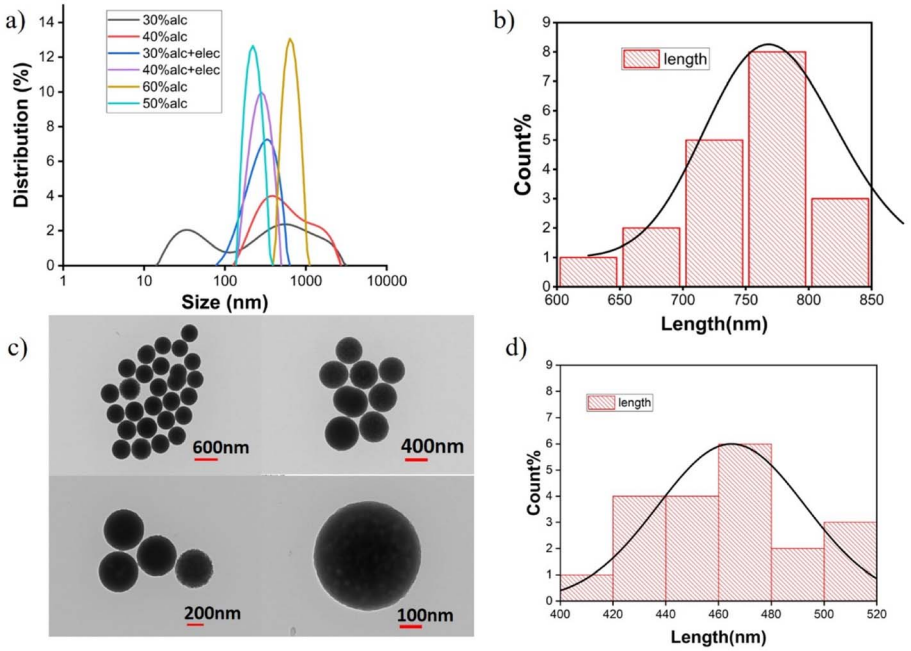

Fig. 3 (a) Particle size distribution (PSD) of different alcoholic concentration systems: 30% and 40% alcohol with electrolyte and without electrolyte; 50%, and 60% alcohol non-electrolyte systems. (b) Histogram of the particle size distribution (PSD) obtained from a TEM study of synthesized particles using 50% ethanol. (c) TEM image of particles synthesized using 67 mM electrolyte and 30% ethanol. (d) Histogram of the particle size distribution (PSD) obtained from a TEM study of particles synthesized using 67 mM electrolyte and 30% ethanol.

homogeneity/monodispersity decreases. The burst nucleation in the 60% alcoholic system leads to a narrow particle size distribution (PSD). When compared to other solvent systems (Fig. 3a), the silicic acid concentration in 60% ethanolic solvent is the highest (Fig. 2a), which helps to increase the silicic acid critical aggregation concentration/supersaturation concentration for burst nucleation. Diluted solvent systems like 30% and 40% alcoholic compositions have problems with the slow primary seed formation, while using an electrolyte brings down the surface charge, *i.e.*, zeta potential (values are given in Table 2) as comparable to 60% and 50% non-electrolytic alcoholic systems, which helps to aggregate the initial hydrolyzed precursor to obtain the CAC. The zeta potential is the electrokinetic potential of colloidal particles and this value indicates the amount of electrostatic repulsion between the same-charged particles. Hence, particles with low zeta potentials have a high tendency toward aggregation.[30]

Particles obtained using the optimized 67 mM electrolyte concentration and 30% ethanol have a characteristic spherical shape (Fig. 3c) with a size range of 400–500 nm. The histogram obtained from the TEM analysis suggests that both the electrolytic and non-electrolytic cases resulted particles with good homogeneity (Fig. 3b, d, and S2 in the ESI†). The 50% ethanol system gives quite larger particles in the 700–800 nm range. This observation and data suggest that using a low organic solvent concentration in conjugation with optimized electrolyte concentration can increase the uniformity of SiNPs. The obtained TEM images also support that the modified composition during the synthesis of SiNP produces particles with comparable size and shape to the previously established method.[16]

3.3. Kinetics study

In the Stöber method, hydrolysis and condensation steps follow first-order kinetics but the overall kinetics is second-order.[24,31] Ammonium hydroxide-mediated Stöber synthesis of SiNP follows the hydrolysis of TEOS through the S_N2 pathway[12] to form monohydroxy alkoxy silane, which upon further hydrolysis gives water-soluble hydroxy silane or monomeric silicic acid.[32,33] These monomeric units after condensation produce dimers, trimers and oligomers. Partially hydrolyzed TEOS also participates in condensation with unhydrolyzed TEOS to form silica nano seeds. All of this form of silica nanoseed is finally condensed to form the SiNP. Aceloin *et al.* studied the kinetics of TEOS hydrolysis using NaOH in a methanol medium using the Karl–Fischer titration method and found that hydrolysis is first-order and depends upon the concentration of TEOS and hydroxyl ions.[34] After hydrolysis, the initial nucleation is quite fast using NaOH as a catalyst.

To establish and support the above-stated mechanism, we investigated the reaction using a kinetics study where we calculated the change in the silicic acid concentration using a molybdate assay. It was a time-limited kinetics study where no such reactant was added during the progress of the reaction. At the very initial stage, when the reaction mixture was free from any primary seed, the silicic acid was collected from the reaction mixture to determine the initial amount, and it was considered the highest concentration. After 2–3 min of reaction, the

Table 1 Variation of rate constant values using different concentrations of electrolyte and solvents

Solvent	Electrolyte	R^2	K (min^{-1})
60% ethanol	Not used	0.96	0.035
50% ethanol	Not used	0.95	0.030
40% ethanol	Not used	0.96	0.023
30% ethanol	Not used	0.88	0.015
40% ethanol	0.034 M	0.93	0.047
30% ethanol	0.068 M	0.95	0.036
30% isopropanol	0.014 M	0.99	0.036

mixture became milky white while stirring and resulted the formation of primary silica seed. This seed generation from different mono-di-oligomeric units and silicic acid produced from unreacted TEOS occurred simultaneously. In this kinetics study, we did not consider the unreacted TEOS as a reactant and assumed that only hydrolyzed TEOS or silicic acid participated in the condensation step. This assumption is quite realistic as –OEt(ethoxy) groups in the partially or unhydrolyzed TEOS inhibited the condensation process by imparting steric hindrance. Our experiments to determine the C_{NP}/C_{SA} (Fig. 2a) suggests that a major concentration change in silicic acid occurs during the initial nucleation, *i.e.*, within 20–30 min, and in the next part of the reaction the generated primary silica nano seed is condensed, followed by nanoparticle synthesis. This statement is also supported by Bhakta *et al.*, who isolated the intermediates during the progress of the reaction and found only the growth of the nanoseeds as long as the reaction continued.[16]

Therefore, the goal was not to study the overall kinetics of the reaction but to establish the effect and benefit of using electrolytes in an alcoholic medium. Hence, we calculated only the rate constant of nucleation or seed formation from silicic acid by using the first-order kinetic model and we got R^2 values of 0.93 and above, which is in the acceptable range (Table 1). The K values suggest that the electrolytic processes are faster than non-electrolytic processes in a 30% ethanol medium. The data further justify our observation and discussed in Section 3.1 about the particle formation using an electrolyte in a 30% alcoholic medium. Further, the kinetics of particle synthesis were compared by using different solvent and electrolyte compositions (Table 1) to determine the effect on reaction rate while changing the composition from 30% ethanol with electrolyte. It was found that the K values for 60% non-electrolyte and 30% electrolyte systems were similar. It was also evident from the rate of formation of particles that a 30% ethanol-electrolyte system is comparable with the high alcoholic composition in terms of producing similar types of nanoparticles.

$$[\text{Silica NP}] = K[\text{silicic acid}] \quad (1)$$

$$k = \frac{1}{t}\ln\left(\frac{C_0}{C_t}\right) \quad (2)$$

C_t = silicic acid conc. at t time, C_0 = initial silicic acid conc., K = rate constant.

The different rate constant data for nanoparticle synthesis in different solvent compositions and also in the presence of electrolytes is given in Table 1.

3.4. The effects of electrolytes

The rate constant data from the kinetic studies suggests that the electrolyte has a significant impact on the nucleation process. In addition, the electrolyte has an important role in particle size determination which was proved while optimizing the electrolyte concentration. The presence of the electrolyte helps to bring down the negative charge of the particle surface and aggregate the monomer particle seeds. Considering one solvent system, 30% ethanol in the presence of 0.080 M NaCl gave particles >1 μm, ζ −30.2 mV, and 0.074 M NaCl led to 800 nm, ζ −31.2 mV, while 0.068 M NaCl produced 307 nm, ζ −31.6 mV particles in DLS measurement. This data explains that a small change in the concentration of electrolyte can reduce the surface potential of particles to an extent, which is enough to decrease the particle size. The Na^+ ions present in the electrolyte decrease the negative surface potential of the particles (Table 2), which decreases the particle–particle repulsion and allows the particles to come in close proximity for agglomeration. Solvents with

Table 2 The variation of size distribution with the polydispersity index (PDI), and the average size, and zeta potential values

Solvent	Electrolyte (M)	PDI (%)	Average hydrodynamic size (nm)	Zeta potential (mV)
60% ethanol	—	4.5	376	−64.4
	0.014	40.5	>1000	−36.4
50% ethanol	—	9.6	237 nm	−47.6
	0.02	27.7	>1000	−33.8
40% ethanol	—	—	No particle was formed	—
	0.034	15.4	309	−39
30% ethanol	—	—	No particle was formed	—
	0.068	26.1	307	−31.6
30% methanol	—	—	No particle was formed	—
	0.068	26.3	270	−29.8
30% isopropanol	—	14.9	158	−62.4
	0.014	2.4	481	−60.1

Table 3 Hydrodynamic sizes and surface zeta-potentials of silica nanoparticles obtained by using different electrolytes

Electrolyte	Electrolyte concentration (mM)	Particle size (nm)	Zeta potential (mV)
LiCl	67	431	−25
NaCl	67	543	−31.2
KCl	67	1226	−52.6
CsCl	67	1679	−66.4

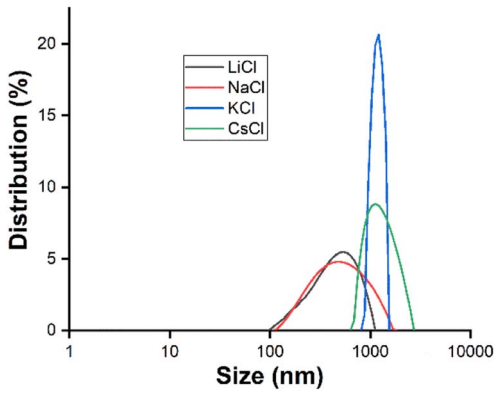

Fig. 4 Size distribution of particles while maintaining 67 mM electrolyte concentration in 30% ethanolic solvent.

low alcohol content slowly attain the supersaturation point. This barrier can be overcome by the addition of an electrolyte because of its substantial ability to decrease the surface charge or zeta potential to aggregate the monomer units and facilitate further seed formation by allowing the unreacted TEOS to be hydrolyzed faster. The overall process ultimately increases the rate constant of SiNP formation. An electrolyte in high concentration generates large particles with high polydispersity, which indicates the non-uniform condensation and aggregation of particles at high electrolytic concentrations.

This is indicated in the zeta potential data given in Table 2, using the same amount of electrolyte in two different solvents, ethanol and methanol, gives particles with different surface potentials; *i.e.*, the change in the zeta potential of a particle is not only governed by the electrolytes but also by solvent polarity.

We tried to understand the role of electrolytes in this aspect. LiCl is generally more covalent compared to NaCl, and similar trends are followed for KCl and CsCl as the size of the cation increases. In addition, since the ionic character increases from LiCl to CsCl, an interesting change in particle size with changing the electrolytes was observed (Table 3). The particle size increased and the surface zeta-potential also became more negative. The increasing ionic character of electrolytes helps to bring down the surface potential in the initial stage of aggregation simply by neutralizing the negative charge of the OH^- ions of silicic acid by counter cationic positive charge and finally forming particles with large sizes; however, the final zeta values are highly negative and they increase with the particle size. This could be due to the higher surface area of larger particles with more available OH^- ions, which is reflected in their zeta potentials (Fig. 4).

3.5. The role of solvent composition on the reaction kinetics and the size of SiNP

Understanding the role of different solvents and solvent mixtures has already been extensively studied in various reports[35,36] but no such details are available on the reaction kinetics and the size while changing solvent compositions. It was already established that the hydrolysis rate constant in the Stöber process increases with the carbon number in the solvent,[37] whereas some of the work has shown that the hydrolysis constant increases with increasing the solvent polarity and decreases with increasing the solvent steric hindrance.[17] In our experiment, NaOH as a base was employed for fast nucleation[16] to initiate the condensation process, *i.e.*, at first the monomer seed generation and its addition to give a final particle upon the condensation process. The kinetic constant data obtained from our process is commensurate with the explanation using the critical aggregation concentration (CAC) theory. TEOS is highly soluble in a solvent where the alcohol content is higher, *i.e.*, 60% alcohol is the best choice in our experimental conditions but the silicic acid is less soluble in this depleted aqueous environment, which actually helps to

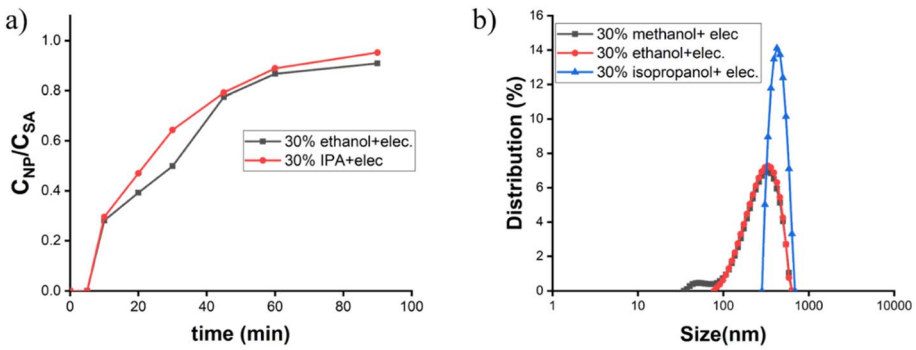

Fig. 5 (a) The concentration changes of silica nanoparticles between the electrolyte-ethanol and electrolyte-isopropanol (IPA) systems. (b) PSD of silica nanoparticles synthesized in 30% methanol, ethanol, and isopropanol with the electrolyte system.

reach the supersaturation concentration of monomer quickly in this solvent system and ultimately leads to the burst nucleation, and this continuous losing and gaining of the supersaturation concentration leads to faster condensation. On diluting the solvent to 30%, the TEOS started phasing out as it became insoluble but the silicic acid produced became more solubilized than other solvent systems, which affected the kinetics of nucleation by the slow gaining of the supersaturation point; *i.e.*, the silicic acid concentration required for supersaturation became higher as it became more soluble in aqueous medium of 30% solvent. The slow monomer seed generation retards the burst nucleation process and the nucleation–condensation kinetics became slow.

Besides 30% ethanol as solvent, the particle nature and size were also compared by varying the solvents, and the average sizes of nanoparticles increased on going from 30% methanol to 30% isopropanol (Fig. 5b). The increasing number of carbons in the solvent and the decreasing polarity correlated well with the observed trend. Isopropanol as the solvent, compared to methanol and ethanol, is less polar having a dielectric constant of 20.4, whereas ethanol and methanol have dielectric constants of 24.5 and 32.7, respectively, at 25 °C.[38] The monomer silicic acid units have less repulsion during monomer aggregation in isopropanol due to the comparatively low polarity of the solvent, which helps to achieve the CAC under lower electrolyte concentration and ultimately leads to burst nucleation. Thus, 30% isopropanol with a comparatively lower electrolytic concentration than 30% ethanol gives almost similar rate constant values (Table 1) for the initial nucleation and a similar kind of change in C_{NP}/C_{SA} values is given in Fig. 5a. The lower concentration of electrolyte reduces the polydispersity (data given in Table 2) in particles with narrow PSD (Fig. 5b) in 30% isopropanol medium.

The higher solvation of reactants than the intermediate can stabilize the reactants and increase the energy barrier of the reaction, which decrease the rate of reaction.[39] The interaction of solvent with reactants and intermediates through H-bonding or complex formation, the calculations of their relative energy, and detailed thermodynamic parameters related to this interaction are beyond the scope of this work. However, we have correlated the solvent properties and their impact on reaction kinetics.

Table 4 Temperature effects on kinetics. Different K values, DLS sizes, and polydispersity indexes (PDI) at different temperatures in the case of 30% alcohol with electrolyte

Temperature (°C)	K (min^{-1})	R^2	Size (nm)	PDI (%)
18	0.01	0.73	657	20.47
28	0.033	0.99	559	12.28
38	0.039	0.95	214	3.60

3.6. The temperature effect on the reaction kinetics and the size of particles

To understand the effect of temperature on the nucleation process, we investigated the silicic acid concentration in the first 30 min by the molybdate assay technique at three different temperatures. The K values were calculated by the simple first-order kinetics of nucleation, where silicic acid was considered as a reactant, and the variation of log C_0/C_t *vs.* time (using eqn (2)) was plotted in a graph and the rate constant (slope value form Fig. 6a) was calculated.

The rate of nucleation increased with every 10 °C temperature increase (Table 4). We measured the average size of those particles and it was evident from Fig. 6b that particles were formed with narrow PSD and a smaller average size at higher temperatures. At higher temperatures, the fast nucleation rate and homogeneity in particle size indicated the quick CAC achievement through the burst nucleation by the solvent system, and there was no such delay between the initial nucleation and particle formation. However, at lower temperatures, the slow nucleation process destroyed the homogeneity in the particle as initial nucleation and particle synthesis from the silicic acid unit occurred simultaneously. Some portion of the early formed silicic acid unit produced large particles, and this inhomogeneity in particle size broadened the PSD and average particle diameter as seen in DLS data. This proved that temperature has an impact on the initial nucleation rate and

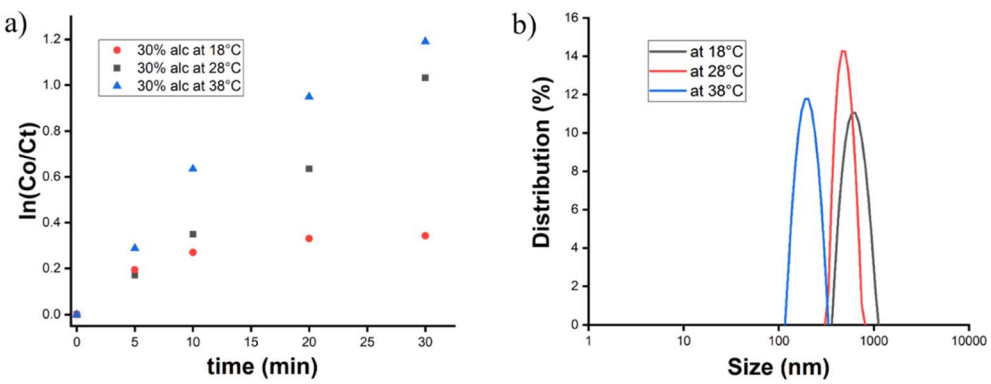

Fig. 6 (a) ln(C_0/C_t) *vs.* time plot for the kinetics study of the nucleation process at 18 °C, 28 °C and 38 °C for 30% alcohol with electrolyte. (b) PDI of silica nanoparticles, synthesized in a 60% ethanol-non-electrolytic system. The temperature variation is 18 °C, 28 °C, and 38 °C. The PDI values decrease with increasing temperature, indicating a narrow size distribution (Fig. S4 in ESI†).

the final particle size determination, which can be used to tune the size of SiNPs. Similarly, we also investigated the effect of temperature on the size and polydispersity of the nanoparticles in the presence of an electrolyte and a similar trend was observed. This trend indicated the importance of these two parameters; the concentration of electrolytes and temperature played a vital role in synthesizing silica nanoparticles with desirable sizes in a lower alcoholic concentration.

3.7. Specific surface area

The surface area imparts an important feature on SiNP use in various applications like dye adsorption, protein binding, drug delivery, *etc.* Generally, mesoporous SiNPs, due to their porous nature, have a very high surface area. Despite having lots of different methods for SiNP synthesis, most are complicated and inconvenient, such as particles synthesized at 650 °C in different time scales producing mesoporous SiNP with BET surface areas of 173 to 527 $m^2 g^{-1}$[40] and a surfactant-free SiNP synthesis from rice husk gives particles between 24–87 nm with maximum BET surface area of 740 $m^2 g^{-1}$.[41] Hence it is a challenge to make non-porous silica nanoparticles with a very high surface area in a robust and convenient way. Our method comprising electrolyte-assisted SiNP synthesis is quite efficient in this matter. Particles in the size range of 400–500 nm showed a very high specific surface area of 1647 $m^2 g^{-1}$ (Table S2 and Fig. S2†). This was obtained by using the Langmuir adsorption isotherm while adsorbing Methylene Blue (MB) dye using different concentrations.[42] Thus, particles synthesized with electrolytes may be more suitable for protein binding, use as sensors, in dye[43] and oil adsorption,[44] and a variety of other applications.[45]

3.8. Cost analysis

We have estimated an overall approximate cost of synthesis of the nanoparticles to envisage the potential in the industrial market. The production cost of SiNPs using 60% ethanol for a small-scale batch of 20 mL is ~20 cents and $10 per liter. In the electrolyte-assisted process where the ethanol concentration is only 30%, the cost for 1 L of silica nanoparticles was reduced to $6 from $10 (up to 35–38%). In the case of large-scale industrial production, the overall cost will be much lower. However, by incorporating electrolytes, it would be much cheaper, as well as environmentally friendly.

4. Conclusion

The correlation between the kinetics of nucleation and growth of the SiNPs has been established and it was found to be linear. The rate of nucleation was slow in the diluted organic solvent composition, however, the rate increased substantially after addition of an electrolyte. It is thus possible to synthesize SiNPs by incorporating electrolytes at a very low concentration in a mixture with less organic solvent. We measured the zeta potential of the nanoparticles and found that a low electrolytic concentration resulted a higher negative surface charge, which accounted for the better colloidal stability in solution. The higher concentration of electrolyte leads to large irregular particles, even in the micron size range, along with very high polydispersity. The final optimized concentration of electrolyte gives particles in the 250–800 nm range. Comparing methanol, ethanol and isopropanol systems, we found that the addition of an electrolyte significantly decreases the surface zeta-potential, which helps to achieve CAC in a relatively shorter time. In this way, it is possible to reduce the organic solvent content in the synthesis process. The overall process is environment-friendly and at the same time, cheaper by ~35% as compared to the conventional methods where 50–60% organic solvents are used. Changes in other parameters like temperature have an impact on particle growth, size, and polydispersity. It is possible to synthesize SiNPs in bulk amounts with size-tunable properties by simply changing the electrolytes and temperature.

Conflicts of interest

The authors claim no conflict of interest for this work.

Acknowledgements

This research is funded by Department of Chemistry, Cooch Behar Panchanan Barma University and authors acknowledge the CRF facility of IITD for TEM images.

References

1 W. J. Stark, P. R. Stoessel, W. Wohlleben and A. J. C. S. R. Hafner, Industrial applications of nanoparticles, *Chem. Soc. Rev.*, 2015, **44**, 5793–5805.
2 I. I. Slowing, B. G. Trewyn, S. Giri and V. Y. Lin, Mesoporous Silica Nanoparticles for Drug Delivery and Biosensing Applications, *Adv. Funct. Mater.*, 2007, **17**, 1225–1236.
3 M. Mathelié-Guinlet, T. Cohen-Bouhacina, I. Gammoudi, A. Martin, L. Beven, M. H. Delville and C. Grauby-Heywang, Silica nanoparticles-assisted electrochemical biosensor for the rapid, sensitive and specific detection of Escherichia coli, *Sens. Actuators, B*, 2019, **292**, 314–320.
4 E. L. Holthoff, D. N. Stratis-Cullum and M. E. Hankus, A Nanosensor for TNT Detection Based on Molecularly Imprinted Polymers and Surface Enhanced Raman Scattering, *Sensors*, 2011, **11**, 2700–2714.
5 X. D. Wang, Z. X. Shen, T. Sang, X. B. Cheng, M. F. Li, L. Y. Chen and Z. S. Wang, Preparation of spherical silica particles by Stöber process with high concentration of tetra-ethyl-orthosilicate, *J. Colloid Interface Sci.*, 2010, **341**, 23–29.
6 T. Matsoukas and E. Gulari, Dynamics of growth of silica particles from ammonia-catalyzed hydrolysis of tetra-ethyl-orthosilicate, *J. Colloid Interface Sci.*, 1988, **124**, 252–261.
7 V. K. LaMer and R. H. Dinegar, Theory, Production and Mechanism of Formation of Monodispersed Hydrosols, *J. Am. Chem. Soc.*, 1950, **72**, 4847–4854.
8 G. H. Bogush and C. F. Zukoski Iv, Studies of the kinetics of the precipitation of uniform silica particles through the

hydrolysis and condensation of silicon alkoxides, *J. Colloid Interface Sci.*, 1991, **142**, 1–18.
9 G. H. Bogush and C. F. Zukoski IV, Uniform silica particle precipitation: An aggregative growth model, *J. Colloid Interface Sci.*, 1991, **142**, 19–34.
10 S. Wong, V. Kitaev and G. A. Ozin, Colloidal Crystal Films: Advances in Universality and Perfection, *J. Am. Chem. Soc.*, 2003, **125**, 15589–15598.
11 K. D. Hartlen, A. P. Athanasopoulos and V. Kitaev, Facile preparation of highly monodisperse small silica spheres (15 to >200 nm) suitable for colloidal templating and formation of ordered arrays, *Langmuir*, 2008, **24**, 1714–1720.
12 Y. Han, Z. Lu, Z. Teng, J. Liang, Z. Guo, D. Wang, M. Y. Han and W. Yang, Unraveling the Growth Mechanism of Silica Particles in the Stöber Method: In Situ Seeded Growth Model, *Langmuir*, 2017, **33**, 5879–5890.
13 C. C. Carcouët, M. W. Van De Put, B. Mezari, P. C. Magusin, J. Laven, P. H. Bomans, H. Friedrich, A. C. C. Esteves, N. A. Sommerdijk, R. A. Van Benthem and G. de With, Nucleation and Growth of Monodisperse Silica Nanoparticles, *Nano Lett.*, 2014, **14**, 1433–1438.
14 T. Ding, L. Yao and C. Liu, Kinetically-controlled synthesis of ultra-small silica nanoparticles and ultra-thin coatings, *Nanoscale*, 2016, **8**, 4623–4627.
15 T. Yokoi, Y. Sakamoto, O. Terasaki, Y. Kubota, T. Okubo and T. Tatsumi, Periodic Arrangement of Silica Nanospheres Assisted by Amino Acids, *J. Am. Chem. Soc.*, 2006, **128**, 13664–13665.
16 C. K. Dixit, S. Bhakta, A. Kumar, S. L. Suib and J. F. Rusling, Fast nucleation for silica nanoparticle synthesis using a sol–gel method, *Nanoscale*, 2016, **8**, 19662–19667.
17 M. T. Harris, R. R. Brunson and C. H. Byers, The base-catalyzed hydrolysis and condensation reactions of dilute and concentrated TEOS solutions, *J. Non-Cryst. Solids*, 1990, **121**, 397–403.
18 O. Malay, I. Yilgor and Y. Z. Menceloglu, Effects of solvent on TEOS hydrolysis kinetics and silica particle size under basic conditions, *J. Sol-Gel Sci. Technol.*, 2013, **67**, 351–361.
19 A. H. Bari, R. B. Jundale and A. A. Kulkarni, Understanding the role of solvent properties on reaction kinetics for synthesis of silica nanoparticles, *Chem. Eng. J.*, 2020, **398**, 125427.
20 D. R. Hristov, E. Mahon and K. A. Dawson, Controlling aqueous silica nanoparticle synthesis in the 10–100 nm range, *Chem. Commun.*, 2015, **51**, 17420–17423.
21 H. Nakabayashi, A. Yamada, M. Noba, Y. Kobayashi, M. Konno and D. Nagao, Electrolyte-Added One-Pot Synthesis for Producing Monodisperse, Micrometer-Sized Silica Particles up to 7 μm, *Langmuir*, 2010, **26**, 7512–7515.
22 S. D. Karande, S. A. Jadhav, H. B. Garud, V. A. Kalantre, S. H. Burungale and P. S. Patil, Green and sustainable synthesis of silica nanoparticles, *Nanotechnol. Environ. Eng.*, 2021, **6**, 1–14.
23 M. F. Zawrah, A. A. El-Kheshen and H. M. Abd-El-Aal, Facile and economic synthesis of silica nanoparticles, *J. Ovonic Res.*, 2009, **5**, 129–133.
24 P. Singh, *et al.*, Green-monodispersed Pd-nanoparticles for improved mitigation of pathogens and environmental pollutant, *Mater. Today Commun.*, 2022, **30**, 103106.
25 S. K. Bhardwaj, *et al.*, Bio-inspired graphene-based nanosystems for biomedical applications, *Nanotechnology*, 2021, **32**, 502001.
26 H. Yang, C. Li, C. Wei, M. Li, X. Li, Z. Deng and G. Fan, Molybdenum blue photometry method for the determination of colloidal silica and soluble silica in leaching solution, *Anal. Methods*, 2015, **7**, 5462–5467.
27 P. R. Pinto, L. C. Mendes, M. L. Dias and C. Azuma, Synthesis of acrylic-modified sol–gel silica, *Colloid Polym. Sci.*, 2006, **284**, 529–535.
28 Y. Liu, Y. Guo, Y. Zhu, D. An, W. Gao, Z. Wang, Y. Ma and Z. Wang, A sustainable route for the preparation of activated carbon and silica from rice husk ash, *J. Hazard. Mater.*, 2011, **186**, 1314–1319.
29 Lu. Ping and Y.-L. Hsieh, Highly pure amorphous silica nano-disks from rice straw, *Powder Technol.*, 2012, **225**, 149–155.
30 S. Samimi, N. Maghsoudnia, R. B. Eftekhari and F. Dorkoosh, Lipid-Based Nanoparticles for Drug Delivery Systems, *Characterization and Biology of Nanomaterials for Drug Delivery*, 2019. pp. 47–76.
31 C. J. Brinker, Hydrolysis and condensation of silicates: Effects on structure, *J. Non-Cryst. Solids*, 1988, **100**, 31–50.
32 S. L. Chen, P. Dong, G. H. Yang and J. J. Yang, Kinetics of formation of monodisperse colloidal silica particles through the hydrolysis and condensation of Tetraethylorthosilicate, *Ind. Eng. Chem. Res.*, 1996, **35**, 4487–4493.
33 R. K. Iler, *The colloid chemistry of silica and silicates*, 1955, vol. 80, 1, p. 86.
34 R. Aelion, A. Loebel and F. Eirich, *J. Am. Chem. Soc.*, 1950, **72**(12), 5705–5712.
35 D. L. Green, J. S. Lin, Y. F. Lam, M. C. Hu, D. W. Schaefer and M. T. Harris, Hydrolysis of Ethyl Silicate, *J. Colloid Interface Sci.*, 2003, **266**, 346–358.
36 T. W. Zerda and G. Hoang, Size, volume fraction, and nucleation of Stober silica nanoparticles, *Chem. Mater.*, 1990, **2**, 372–376.
37 S. Sadasivan, A. K. Dubey, Y. Li and D. H. Rasmussen, Effect of solvents on the hydrolysis reaction of tetramethyl orthosilicate, *J. Sol-Gel Sci. Technol.*, 1998, **12**, 5–14.
38 G. E. McManis, M. Neal Golovin and M. J. Weaver, Role of solvent reorganization dynamics in electron-transfer processes. Anomalous kinetic behavior in alcohol solvents, *J. Phys. Chem.*, 1986, **90**, 6563–6570.
39 X. Liu, J. Xie, J. Zhang, L. Yang and W. L. Hase, Alcoholic solvent effect on silica synthesis—NMR and DLS investigation, *J. Phys. Chem. Lett.*, 2017, **8**, 1885–1892.
40 S. A. Martell, Y. Lai, E. Traver, J. MacInnis, D. D. Richards, S. MacQuarrie and M. Dasog, Steric Effects of Solvent Molecules on SN2 Substitution Dynamics, *ACS Appl. Nano Mater.*, 2019, **2**, 5713–5719.
41 S. Song, H. B. Cho and H. T. Kim, High Surface Area Mesoporous Silicon Nanoparticles Prepared via Two-Step

Magnesiothermic Reduction for Stoichiometric CO2 to CH3OH Conversion, *J. Ind. Eng. Chem.*, 2018, **61**, 281–287.

42 D. O. Kra, P. Atheba, P. Drogui and A. Trokourey, Surfactant-free synthesis of high surface area silica nanoparticles derived from rice husks by employing the Taguchi approach Preparation and Characterization of Activated Carbon Based on Wood (Acacia auriculeaformis, Côte d'Ivoire), *J. Encapsulation Adsorpt. Sci.*, 2019, **9**, 63.

43 S. A. Jadhav, H. B. Garud, A. H. Patil, G. D. Patil, C. R. Patil, T. D. Dongale and P. S. Patil, Recent advancements in silica nanoparticles based technologies for removal of dyes from water, *Colloid Interface Sci. Commun.*, 2019, **30**, 100181.

44 H. Kesarwani, S. Sharma and A. Mandal, Application of Novel Colloidal Silica Nanoparticles in the Reduction of Adsorption of Surfactant and Improvement of Oil Recovery Using Surfactant Polymer Flooding, *ACS Omega*, 2021, **6**, 11327–11339.

45 P. G. Jeelani, P. Mulay, R. Venkat and C. Ramalingam, A review. Multifaceted application of silica nanoparticles. A review, *Silicon*, 2020, **12**, 1337–1354.